RAPID COMMUNICATIONS

PHYSICAL REVIEW C VOLUME 48, NUMBER 5 NOVEMBER 1993

Particle-drip lines from the Hartree-Fock-Bogoliubov theory with Skyrme interaction

R. Smolańczuk
Sołtan Institute for Nuclear Studies, Hoża 69, 00-681 Warsaw, Poland
J. Dobaczewski
Institute of Theoretical Physics, Warsaw University, Hoża 69, 00-681 Warsaw, Poland
(Received 15 July 1993)

We calculate positions of one- and two-particle, proton and neutron drip lines within the Hartree-Fock-Bogoliubov theory using Skyrme interaction. We also determine an approximate r-process path defined as a line where the neutron binding energy is equal to 2 MeV. A weakening of the nuclear shell structure at drip lines is found and interpreted as resulting from a coupling with continuum states.

PACS number(s): 21.60.Jz, 21.10.Dr

A description of nuclei far from the stability line is one of the most important challenges for the nuclear structure theory. Various methods of extrapolating measured nuclear masses to large neutron or proton excess have already been proposed [1]. The proton-drip line has been reached and crossed experimentally in several places of the nuclear chart. On the other hand, the neutron-drip line has been experimentally reached only for very light nuclei. Its exact position for heavier nuclides is still not known and theoretical predictions [1] may differ by as much as 12 mass units for Z=50.

In the present study we report on calculations determining the proton and neutron, one- and two-particle drip lines by using the self-consistent mean-field approach. Since the position of one-particle-drip lines depends crucially on a cancellation between mean-field and pairing effects, the complete Hartree-Fock-Bogoliubov (HFB) equations [2] have to be solved, which allow for a correct description of the interplay between particle-particle and particle-hole channels of interaction. We use here the HFB theory with Skyrme interaction [3].

The HFB method has an advantage of giving nuclear density which goes to zero at large distances, even for nuclei having Fermi energy arbitrarily close but below zero. At the same time, when it is solved in the coordinate space it fully takes into account the coupling of bound states to continuum [3]. In this way one avoids the appearance of unphysical particle gas which would surround the nucleus if the BCS approximation had been used to describe pairing correlations. The HFB method has recently been used [4] to describe properties of nuclei far from stability constituting the neutron-star crust.

Many different parametrizations of the Skyrme force existing in the literature have been obtained by fitting properties of known nuclei. Apart from standard versions [5,6] used in various nuclear structure calculations, there are recently numerous attempts to obtain improved parameters. A large-scale adjustment of parameters to many nuclear masses has been possible by using the extended Thomas-Fermi approximation to the Hartree-Fock (HF) method [7], and the particle-drip lines have been determined in this way. A force devised for a description of nuclei far from stability has been obtained [8] by fitting the Skyrme energy functional to the free energy of nuclear and neutron matter calculated using hyper-netted chain techniques. Improved parametrizations have been found in the seniority HF calculations [9]. The particle-drip lines have also been estimated from the relativistic Hartree theory [10].

An extrapolation to nuclei far from stability can be meaningful only if the force parametrization is used within the same theoretical method where it has been determined. Unfortunately, the numerical effort of the HFB calculations is large, and a large-scale fitting of parameters is still unavailable. Moreover, both the fitting and the extrapolation should be made by using deformed HFB codes in the coordinate space which do not yet exist. In this study we present a pilot calculation within the spherical approximation to the HFB method as described in Ref. [3], and we use the SkP force parametrization, which has been obtained there by fitting properties of several magic nuclei together with the Z=50 isotopic chain.

For fixed proton number Z, the neutron-drip line separates the heaviest even-N nucleus from the next odd-N isotope such that the neutron separation energy S_n is negative,

$$S_n \equiv E^{\rm even}(N) - E^{\rm odd}(N+1) < 0, \qquad (1)$$

where $E^{\rm even}(N)$ and $E^{\rm odd}(N+1)$ denote ground-state energies of neighboring even and odd isotopes, respectively. In the HFB theory the number of particles is not conserved and the energy is a function of the Lagrange multiplier λ called the Fermi energy. By changing λ we may obtain HFB solutions with arbitrary (not necessarily integer) average particle numbers. Since the HFB variational wave function contains only even-particle-number components, the usual HFB solutions describe even nuclei even if the average particle number N is odd or not integer at all. We denote the ground-state energies obtained in this way by $\tilde{E}^{\rm even}(\lambda)$.

In order to describe odd nuclei one should in principle use variational function containing only odd-particle-number components. Usually one avoids this step by using the so-called blocking approximation [2]. In the present study we still simplify the calculations by approximating ground-state energies of odd nuclei as

$$\tilde{E}^{\rm odd}(\lambda) \simeq \tilde{E}^{\rm even}(\lambda) + \min_{\mu} E_{\mu}(\lambda), \qquad (2)$$

where $E_\mu(\lambda)$ are the quasiparticle energies obtained in the HFB theory for a given value of λ. As shown in Ref. [3], this is a fair approximation to the blocking approach.

Because in the HFB theory the neutron number is a continuous variable, we may fulfill the one-neutron-drip-line condition (1) by looking for such two values of the Fermi energy λ and λ' that

$$\tilde{E}^{\rm even}(\lambda') - \tilde{E}^{\rm odd}(\lambda) = 0 \tag{3}$$

and $N(\lambda')=N(\lambda) - 1$. On the other hand, in the HFB theory the Fermi energy is rigorously equal to the derivative of ground-state energy with respect to the particle number,

$$\lambda = \frac{\partial \tilde{E}^{\rm even}(N)}{\partial N}, \tag{4}$$

and we may use the following first-order Taylor expansion:

$$\tilde{E}^{\rm even}(N') \simeq \tilde{E}^{\rm even}(N) + (N' - N)\frac{\partial \tilde{E}^{\rm even}(N)}{\partial N}, \tag{5}$$

which gives

$$\tilde{E}^{\rm even}(\lambda') \simeq \tilde{E}^{\rm even}(\lambda) - \lambda. \tag{6}$$

Inserting approximations (2) and (6) to the one-neutron-drip-line condition (3) one obtains

$$\lambda + \min_\mu E_\mu(\lambda) = 0, \tag{7}$$

and this condition has been used in the calculations of the present study.

The advantage of using such a condition consists in avoiding all explicit calculations for odd nuclei as well as constraints for neutron number N. Once the HFB equations are solved under condition (7) we can calculate the (not necessarily integer) neutron number $N(\lambda)$ corresponding to the obtained Fermi energy λ. We then establish the one-neutron-drip line as passing between the even isotope closest to the obtained neutron number $N(\lambda)$ and the next heavier odd isotope. With this prescription and approximations (2) and (6) one can determine the position of the drip line with a precision of ± 2 mass units.

Outside the one-neutron-drip line all odd isotopes are unstable, whereas the even ones are stable up to the two-neutron-drip line defined by

$$S_{2n} \equiv E^{\rm even}(N) - E^{\rm even}(N+2) < 0, \tag{8}$$

where S_{2n} is the two-neutron separation energy, and $E^{\rm even}(N)$ and $E^{\rm even}(N+2)$ denote ground-state energies of neighboring even isotopes, respectively. Considerations similar to those presented above allow us to approximate condition (8) by the HFB equations solved under the condition

$$\lambda = 0. \tag{9}$$

This corresponds to simply omitting the neutron-number constraint when solving the HFB equations. Of course, the constraint on proton number always must be present when using conditions (7) or (9) because it defines the number of protons Z at which we determine the positions of neutron-drip lines. In order to obtain the positions of proton-drip lines we may repeat *mutatis mutandis* all above considerations.

In our numerical calculations the neutron-drip lines have been determined for even Z between Z=8 and 124, and the proton-drip lines for even N between N=8 and 210, i.e., well beyond the fission instability limits. An overview of the results is presented in Fig. 1 where the scale is large enough that one can read off the exact positions of drip lines from the Fig. 1. The convention used is that of a nuclear chart, i.e., the even-even nuclides are represented by squares delimited by the pairs of tics on the abscissa and on the ordinate. Longer tics show limits of squares for particle numbers divisible by 20. The lines in Fig. 1 separate squares corresponding to stable and unstable nuclides.

The influence of closed major shells on proton-drip lines is clearly visible at Z=50, 82, and 126. At these proton numbers the one- and two-proton-drip lines coincide and have long horizontal sections centered around N=50, 104, and 194, respectively. This corresponds to closed proton shells to which adding neither one nor two protons can produce a stable nucleus. At large Z, the proton shell structure at proton-drip lines is therefore the same as that for stable nuclei. On the other hand, for smaller proton numbers the shell structure is not visible at proton drip lines.

Similar effects are seen in Fig. 2 where we present the average proton pairing gap Δ_p [3] and the binding energy per particle B/A calculated along the one-proton-drip line as functions of the proton number. At large proton magic numbers Z=50, 82, and 126 the pairing correlations disappear and the binding energy sharply increases. At lower magic numbers the pairing correlations decrease but do not vanish, while the binding energy has wide maxima, which is a signature of a less pronounced shell structure. On the other hand, at the one-neutron-drip line (i.e., when protons are deeply bound) the proton pairing gap vanishes at every usual magic number, Fig. 2.

A weakening of the shell structure at neutron-drip lines is manifest when looking at the results presented in Fig. 1. Neither one- nor two-neutron-drip lines have long vertical sections at constant N values corresponding to usual magic numbers. Only wide bends are seen around N=126, 184, and 258, which are the magic numbers of the spherical shell model. They illustrate the remaining influence of the shell structure in nuclei with very large neutron excess.

This is confirmed by the behavior of the neutron pairing gap Δ_N and of the binding energy along the neutron-drip line, Fig. 3. The weakness of a shell effect at N=82 is especially striking. It can probably be attributed to a modified position of the $1h_{11/2}$ orbital, which at the neutron-drip line is located in the middle of the N=82 shell gap. This supports the suggestion [11] that the spin-orbit splitting may be smaller at large neutron excess, because a larger surface diffuseness may lead to a decreased strength of the spin-orbit interaction form factor. In fact, it would also be very interesting to determine the spin-orbit strength at large neutron excess, which can be done in the frame of the relativistic Hartree-Fock theory [12,13], and see whether it may modify the position

of intruder states at the neutron-drip line.

In Fig. 1 we also present the results of the HFB calculations with the neutron Fermi energy being fixed at the value of 2 MeV. This roughly corresponds to the approximate r-process path [14], which should pass through nuclei which are at the origin of the abundance maxima. Available experimental information about the r-process path suggests that it should pass through nuclides $^{80}_{30}Zn_{50}$, $^{130}_{48}Cd_{82}$, and $^{195}_{69}Tm_{126}$ which in Fig. 1 are shown as full squares.

Our approximate r-process path goes through $^{195}_{69}Tm_{126}$ at N=126, where a vertical section of the path reappears. This illustrates an increased role of the shell structure when one moves away from the drip lines and when the coupling with continuum states decreases. On the other hand, such vertical sections do not reappear at

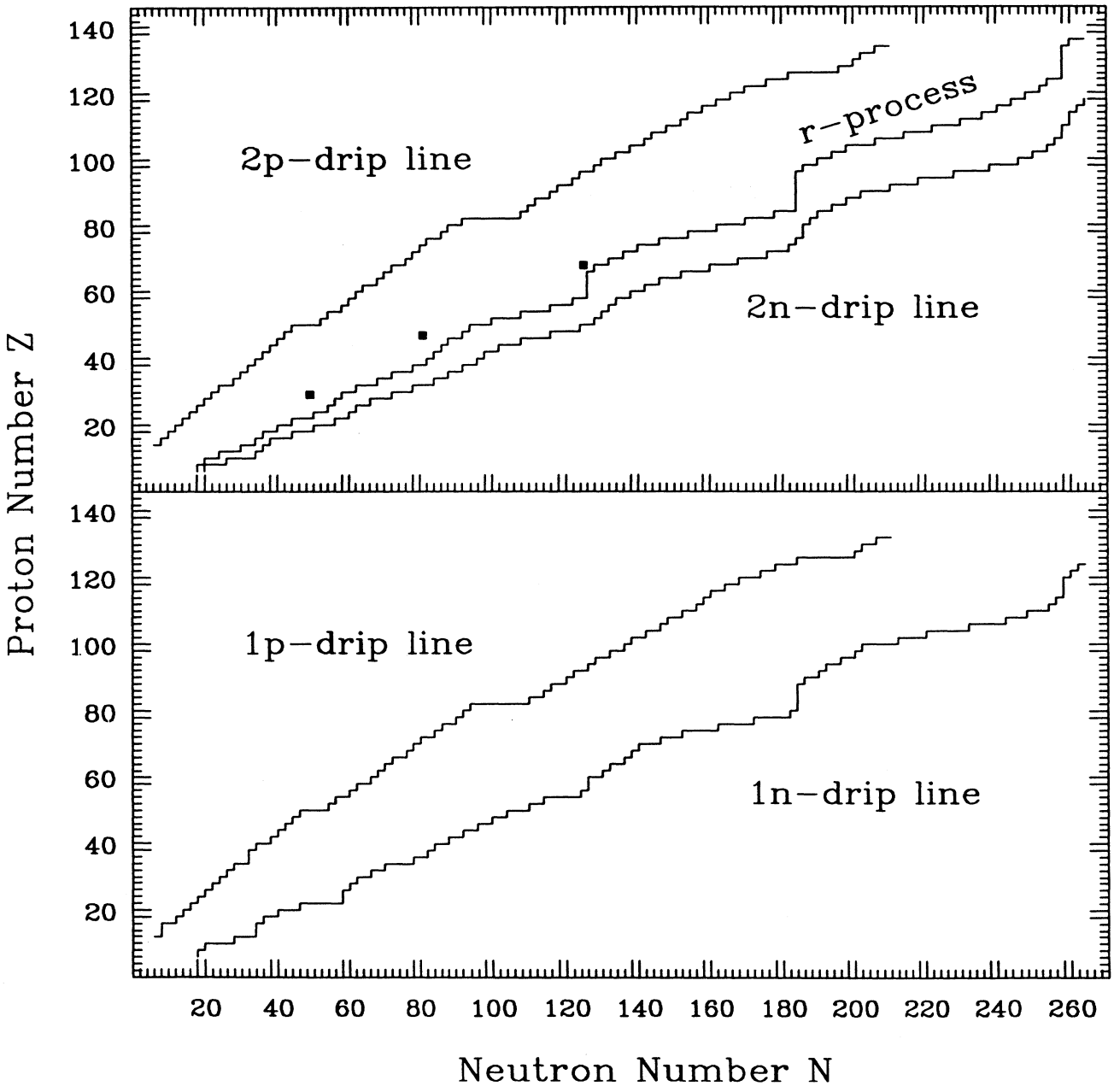

FIG. 1. One-particle (bottom) and two-particle (top) neutron and proton drip lines obtained within the HFB theory with the SkP Skyrme interaction. The middle line in the top part of the figure corresponds to an approximated r-process path. Three full squares represent positions of the three nuclides being at the origin of abundance maxima, i.e., $^{80}_{30}Zn_{50}$, $^{130}_{48}Cd_{82}$, and $^{195}_{69}Tm_{126}$.

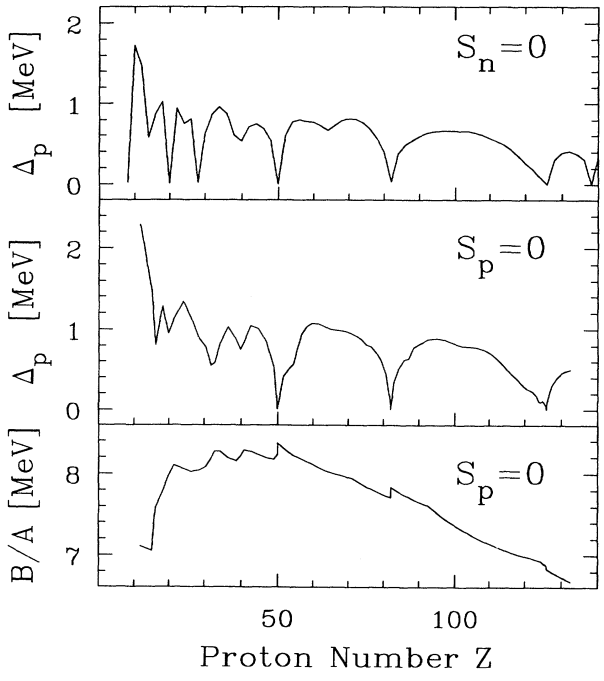

FIG. 2. Binding energy per particle B/A (bottom) and the proton pairing gap Δ_p (middle) calculated at the one-proton-drip line as a function of the proton number Z. The proton pairing gap Δ_p calculated at the one-neutron-drip line is also shown (top).

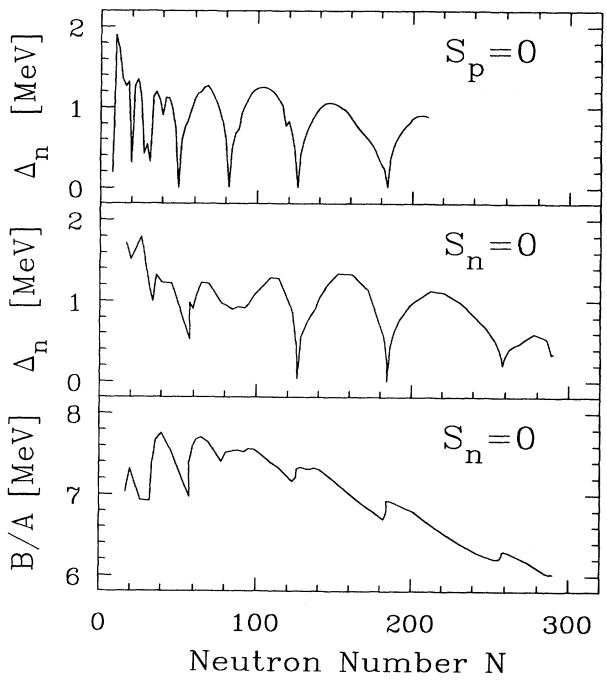

FIG. 3. Same as in Fig. 2, but for neutrons.

N=50 and 82, and our r-process path misses the nuclides $^{80}_{30}Zn_{50}$, $^{130}_{48}Cd_{82}$ by a few mass units. However, dynamic reaction networks r-process calculations with the HFB masses should be performed if one wants to properly assess the validity of the force parameters at large neutron excess [15].

In conclusion, the HFB calculations with the SkP Skyrme force performed within the spherical approximation for nuclei with large proton or neutron excess indicate that the shell structure at magic particle numbers is weaker than that in stable nuclei. This effect can be attributed to the pairing interaction with the continuum states taken into account in the HFB method. The detailed positions of particle drip lines may certainly be affected by the deformation effects. Therefore, the spherical HFB analysis presented here should be extended to a model allowing for various spatial deformations, and the work along this line is now in progress.

We gratefully acknowledge helpful discussions with P. Haensel and A. Sobiczewski. This research was supported in part by the Polish State Committee for Scientific Research under Contracts No. 20450 91 01 and No. 20954 91 01.

[1] P.E. Haustein (special editor), At. Data Nucl. Data Tables **39**, 185 (1988).
[2] P. Ring and P. Schuck, *The Nuclear Many-Body Problem* (Springer-Verlag, New York 1980).
[3] J. Dobaczewski, H. Flocard, and J. Treiner, Nucl. Phys. **A422**, 103 (1984).
[4] P. Haensel, J.L. Zdunik, and J. Dobaczewski, Astron. Astrophys. **222**, 353 (1989).
[5] M. Beiner, H. Flocard, Nguyen van Giai, and P. Quentin, Nucl. Phys. **A238**, 29 (1975).
[6] J. Bartel, P. Quentin, M. Brack, C. Guet, and H.-B. Håkansson, Nucl. Phys. **A386**, 79 (1982).
[7] Y. Aboussir, J.M. Pearson, A.K. Dutta, and F. Tondeur, Nucl. Phys. **A549**, 155 (1992).
[8] V.J. Pandharipande and D.G. Ravenhall, in *Proceedings of a NATO Advanced Research Workshop on Nuclear Matter and Heavy Ion Collisions*, Les Houches, 1989, edited by M. Soyeur (Plenum, New York, 1989), p. 103.
[9] J.M.G. Gómez, C. Prieto, and J. Navarro, Nucl. Phys. **A549**, 125 (1992).
[10] D. Hirata, H. Toki, T. Watabe, I. Tanihata, and B.V. Carlson, Phys. Rev. C **44**, 1467 (1991).
[11] C.J. Pethick and D.G. Ravenhall, in *Neutron Stars: Theory and Observation*, edited by J. Ventura and D. Pines, NATO ASI Series C: Vol 334 (Kluwer, Dordrecht, 1991) p. 3; Report No. NORDITA - 91/24 AN (unpublished).
[12] P.-G. Reinhard, M. Rufa, J. Maruhn, W. Greiner, and J. Friedrich, Z. Phys. A **323**, 13 (1986).
[13] M. Rufa, P.-G. Reinhard, J.A. Maruhn, W. Greiner, and M.R. Strayer, Phys. Rev. C **38**, 390 (1988).
[14] J.J. Cowan, F.-K. Thielemann, and J.W. Truran, Phys. Rep. **208**, 267 (1991).
[15] C.E. Rolfs and W.S. Rodney, *Cauldrons in the Cosmos* (The University of Chicago Press, Chicago, 1988)